Experimental Thermal and Fluid Science 33 (2009) 472–481

Contents lists available at ScienceDirect

Experimental Thermal and Fluid Science

journal homepage: www.elsevier.com/locate/etfs

Experimental analysis of microwave heating of dielectric materials using a rectangular wave guide (MODE: TE_{10}) (Case study: Water layer and saturated porous medium)

Waraporn Cha-um, Phadungsak Rattanadecho *, Watit Pakdee

Research Center of Microwave Utilization in Engineering (RCME), Department of Mechanical Engineering, Faculty of Engineering, Thammasat University (Rangsit Campus), Paholyothin, Pathumthani 12120, Thailand

ARTICLE INFO

Article history:
Received 6 June 2008
Accepted 16 November 2008

Keywords:
Microwave heating
Rectangular wave guide
Porous medium

ABSTRACT

The heating process of dielectric materials by microwave with rectangular wave guide has been investigated experimentally. This experiment is operated in the TE_{10}-dominated mode at a frequency of 2.45 GHz. It was performed for two dielectric materials, water layer and saturated porous medium. In this work, the microwave powers level, a type of dielectric materials, dimensions and positions of dielectric material on the microwave power absorb and average temperature within dielectric materials were examined in details. The results show that the locations of sample have greater effects than the other parameters. The analyses from this research serve as essential fundamentals to development of mathematic models of heat and mass transfer phenomena.

1. Introduction

Microwave heating is one of the most interesting methods for heating materials. Unlike other heat sources such as conventional heating, where heat is applied externally to the surface of the material, microwave irradiation penetrates and simultaneously heats the bulk of the material. Microwave technology has several advantages over conventional mechanical methods, such as minimizing the heating times, uniform temperature distribution, high energy efficiency, and offer improvements in product quality for various industrial fields. Many successful examples of this application, including the drying of foods, drying of textiles, freeze drying process, and vulcanizations of rubber.

Refer to Metaxas and Meridith [1] and Saltiel and Datta [2] for an introduction to heat and mass transfers in microwave processing. Other important papers addressing modeling of microwave-heating processes include Ayappa et al. [3], Clemens and Saltiel [4], Dibben and Metaxas [5], Zhao and Turner [6], Bows et al. [7], Zhao et al. [8], Watanuki [9], Basak and Ayappa [10] and Ratanadecho et al. [11–13].

Although most of previous investigations considered simulations of microwave heating in solid sample, a little effort has been reported on study of multi-dimensional heating process of liquid layer by microwave fields, especially, full comparison between mathematical simulation results with experimental heating data.

A study of microwave heating of liquid was investigated by many researchers. The earliest studies, for example, Lenz [14], have used a lumped parameter approach in modeling microwave heating of liquids. A study of natural convection in a liquid expose to microwave was studied by Datta et al. [15] which the microwave power absorbed was assumed to decay exponentially into the sample following the aid of Lambert's law. However, this assumption is valid only for the large sample dimensions and high loss dielectric materials. The important paper addressing modeling of microwave driven convection in square cavity exposed to waves from different directions was made by Ayappa et al. [3]. A study of microwave induced natural convection in 3D was made by Zhang et al. [16]. The model solved the Maxwell's equation in 3D using the FDTD method and solved the flow field for distilled water and corn oil. Ratanadecho et al. [13] were the first who investigated, numerically and experimentally, for microwave heating of liquid layer with different dielectric properties using a rectangular wave guide. The movement of liquid induced by microwave energy was taken into account. Coupled electromagnetic, hydrodynamic and thermal field were simulated in two dimensions. The spatial variation of electromagnetic field was obtained by solving Maxwell's equations with the FDTD method. Their work demonstrated the effects of microwave power level and liquid dielectric properties on the degree of penetration and rate of heat generation within the liquid layer. The simulated results were validated by comparing with experimental results. Recently, microwave heating of liquid flowing in a rectangular duct passing through the cubic cavity was study by Zhu et al. [17]. The effects of the diameter of applicator tube and the shape of microwave cavity were investigated. The

* Corresponding author. Tel.: +66 0 2564 3001x9; fax: +66 0 2564 3010.
E-mail address: ratphadu@engr.tu.ac.th (P. Rattanadecho).

0894-1777/$ - see front matter © 2008 Elsevier Inc. All rights reserved.
doi:10.1016/j.expthermflusci.2008.11.008

microwave heating of liquid inside rotating container was numerically study by Chatterjee et al. [18], in which, the effects of the various parameters, namely the rotational forces, power source intensity and the gravitational forces, on the microwave heating of containerized liquids in the presence of rotating turntables were investigated.

The other microwave heating in nowadays, Rattanadecho [19] presented a two dimensional numerical model to predict the distribution of electromagnetic fields, power and temperature profiles within wood that located in rectangular wave guide. Basak and Ayappa [20] showed the microwave thawing of 2D frozen cylinders where the uniform plane wave was irradiated on one face.

However, except in the studies by Ratanadecho et al. [11–13], a little effort has been reported on experimental study of microwave heating of liquid layer or microwave heating of a fluid-saturated porous packed bed in detail. Due to the limited amount of theoretical and experimental work on microwave heating of dielectric materials, i.e., liquid layer and fluid-saturated porous packed bed reported to date, the various effects are not fully understood and numbers of critical issues remain unresolved. These effects of reflection rate of microwave, the variation of microwave power level, dimension and position of sample and dielectric properties during microwave heating of dielectric materials have not been systematically studied. Generally the variation of the microwave power level, dimension and position of sample and change of dielectric properties during microwave heating of dielectric materials could change the degree of penetration and rate of heat generation within the heating layer. The reflection rate of microwave strongly depends on the dielectric properties of the heating layer so that the effects of the variation of microwave power level, dimension and position of sample and dielectric properties and must be considered in this work.

This study reports an experimental data during microwave heating of dielectric materials i.e., liquid layer and saturated porous packed bed using a rectangular waveguide in which the microwave of TE_{10} mode operating at a frequency of 2.45 GHz is employed.

2. Related theories

With the basic knowledge of heating by microwave energy, it concerns heat dissipation and typical microwaves propagation the basic equation to calculate the density of microwave power absorbed by dielectric material (Q) can be here below established [13]

$$Q = \omega\varepsilon_0\varepsilon_r'' E^2 = 2\pi \cdot f \cdot \varepsilon_0 \cdot \varepsilon_r'(\tan\ \delta)E^2 \quad (1)$$

where E is electromagnetic field intensity; f is microwave frequency; ω is angular velocity of microwave; ε_r' is relative dielectric constant; ε_0 is dielectric constant of air and tan δ is dielectric loss tangent coefficient.

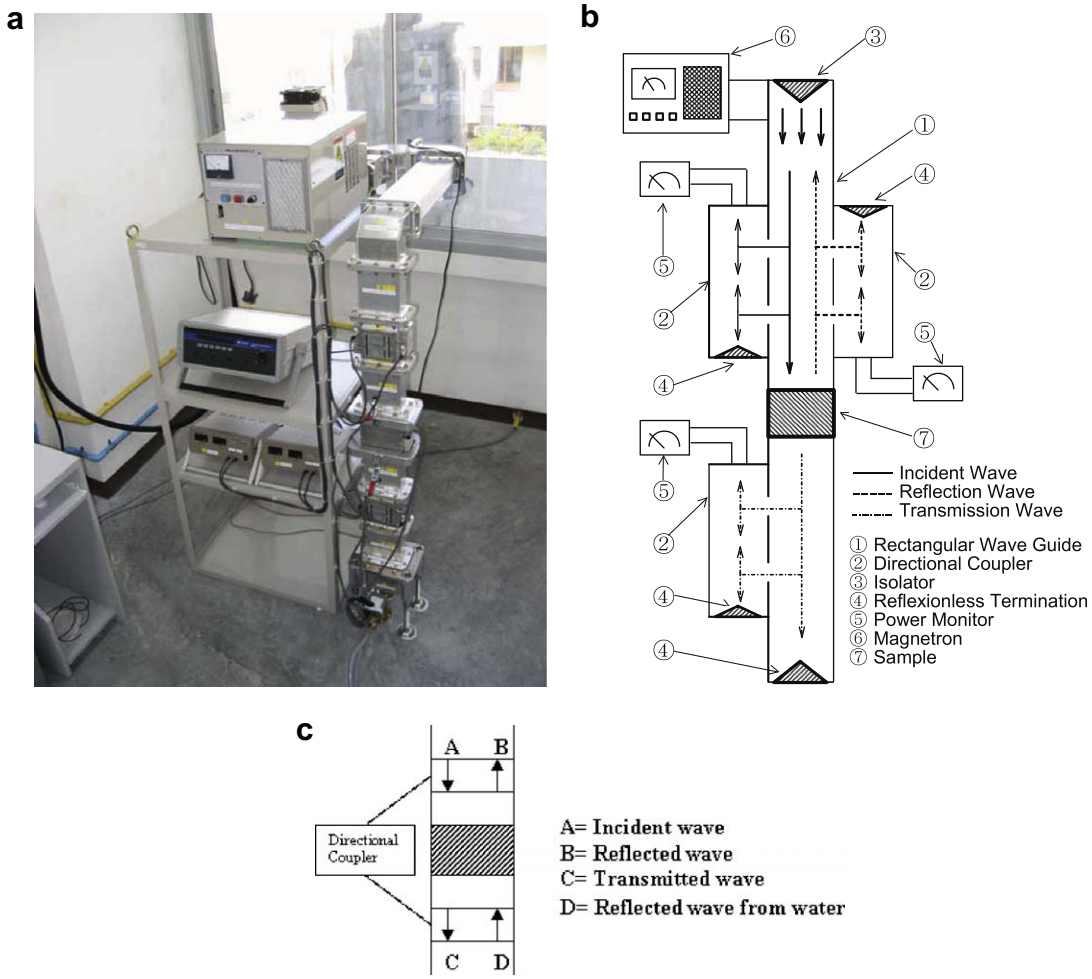

Fig. 1. Schematic of experimental facility: (a) equipment setup; (b) microwave measuring system; (c) microwave power measuring.

From Eq. (1), Q is directly proportional to the frequency of the applied electric field and dielectric loss tangent coefficient and root-mean-square value of the electric field. It means that increasing of tan δ of sample, absorption of microwave energy and generated heat are also increased. While tan δ is small, microwave will penetrate into sample without heat generation. However, the temperature increasing is probably depending on other factors such as specific heat, size and characteristic of sample.

When the material is heated unilaterally, it is found that as the dielectric constant and loss tangent coefficient vary, the penetration depth will be changed and the electric field within the dielectric material is altered. The penetration depth is used to denote the

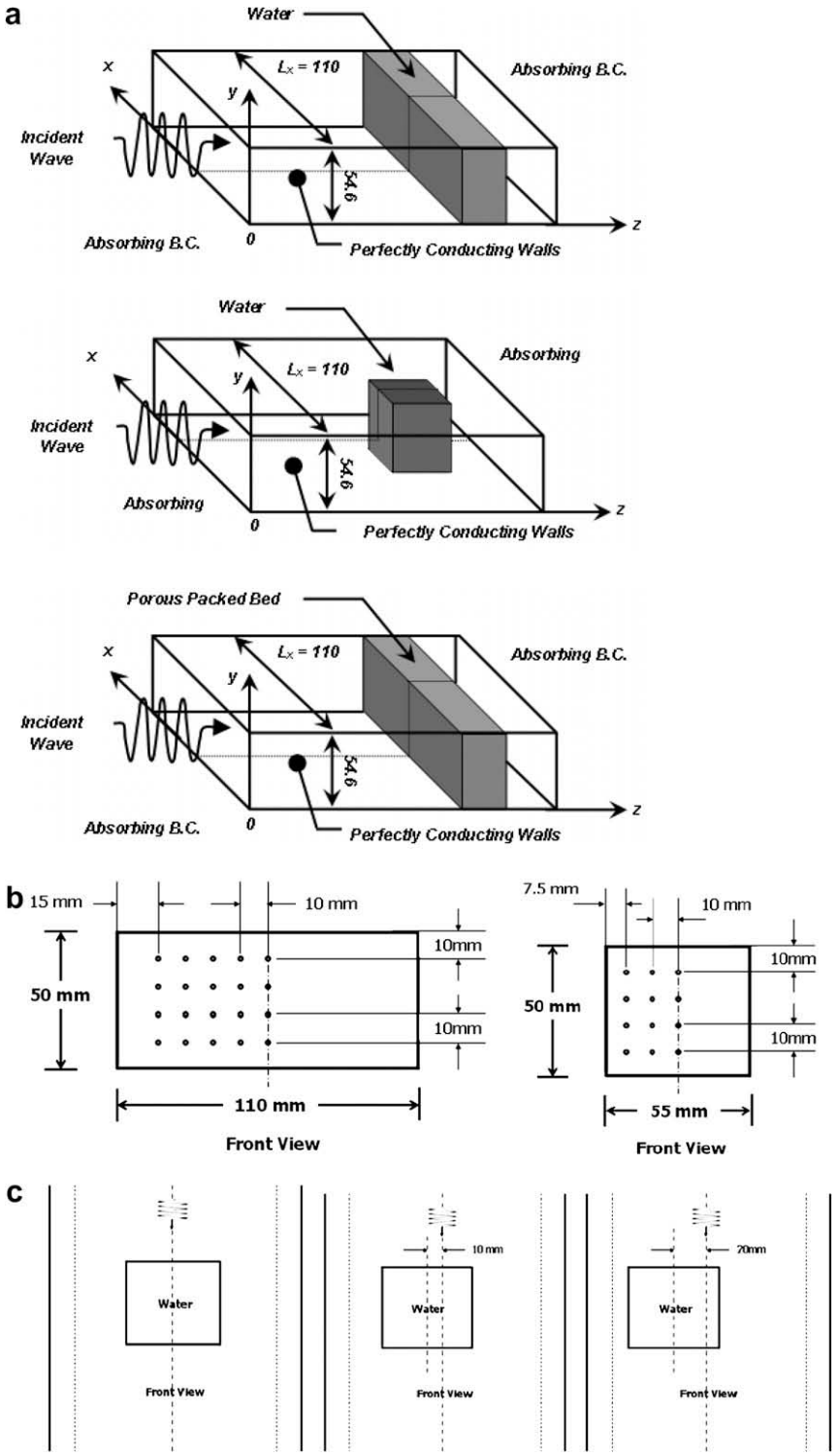

Fig. 2. Schematic of experimental analysis: (a) analysis model; (b) locations of temperature measurement in symmetrical plane; (c) positions of sample inside wave guide.

depth at which the power density has decreased to 37% of its initial value at the surface [13]

$$D_p = \frac{1}{\frac{2\pi f}{\upsilon}\sqrt{\frac{\varepsilon_r'\left(\sqrt{1+\left(\frac{\varepsilon_r''}{\varepsilon_r'}\right)^2}-1\right)}{2}}} = \frac{1}{\frac{2\pi f}{\upsilon}\sqrt{\frac{\varepsilon_r'(\sqrt{1+(\tan\ \delta)^2}-1)}{2}}} \quad (2)$$

where D_P is penetration depth, ε_r'' is relative dielectric loss factor. And υ is microwave speed. The penetration depth of the microwave power is calculated according to Eq. (2), which shows how it depends on the dielectric properties of the material. It is noted that products with huge dimensions and high loss factors, may occasionally overheat a considerably thick layer on the outer layer. To prevent such phenomenon, the power density must be chosen so that enough time is provided for the essential heat exchange between boundary and core. If the thickness of the material is less than the penetration depth, only a fraction of the supplied energy will become absorbed. In example, consider the dielectric properties of water typically show moderate lousiness depending on the temperature. The water layer at low temperature typically shows slightly greater potential for absorbing microwaves. In the other word, an increase in the temperature typically decreases ε_r'', accompanied by a slight increment in D_p.

3. Experimental apparatus

In the present study, the experimental analysis of heat transfer in dielectric material is conducted. Fig. 1a shows the experimental apparatus. The microwave system is a monochromatic wave of TE_{10} mode operating at a frequency of 2.45 GHz. Microwave is generated by magnetron, it is transmitted along the z-direction of the rectangular wave guide with inside dimensions of 110×54.61 mm^2 toward a water load that is situated at the end of the wave guide. Fig. 1b shows the water load (lower absorbing boundary) which ensures that only a minimal amount of microwave is reflected back to the sample. The warm water load from microwave system is circulated through the cooling tower in order to reject heat to ambient. On the upstream side of the sample, an isolator is used to trap any microwave reflected from the sample to prevent the microwave from damaging the magnetron. The powers of incident, reflected and transmitted waves are measured by a wattmeter using a directional coupler (MICRO DENSHI., model DR-5000). Fiberoptic (LUXTRON Fluroptic Thermometer., model 790, accurate to ±0.5 °C) is employed for temperature measurement. The fiberoptic probes are inserted into the sample, and situated on the XZ plane at $Y = 25$ mm. Due to the symmetrical condition, temperatures are measured for only one side of plane as illustrated in Fig. 2b. An initial temperature of sample is 28 °C for all cases. A summary of the experimental procedure is depicted by Fig. 4. Samples considered are water layer and saturated porous packed bed that composes of glass beads (diameter of 0.15 mm with a porosity of 0.385.) filled with water. Different dimensions of samples in the x–z-direction are detailed in Fig. 2a. A sample container with a thickness of 0.75 mm is made from polypropylene which does not absorb microwaves. The samples will be heated by the microwave system that produces a monochromatic wave of TE_{10} mode having a frequency of 2.45 GHz. The dielectric properties for samples were measured at 28 °C using a portable dielectric measurement (Network Analyzer) over a frequency band of 1.5–2.6 GHz as shown in Fig. 3. The portable dielectric measurement kit allows for measurements of the complex permittivity over a wide range of solid, semi-solid, granular and liquid materials. It performs all of the necessary control functions, treatment of the microwave signals, calculation, data processing, and results representation. The software controls the microwave reflectometer to measure the complex reflection coefficient of the material under test (MUT). Then it detects the cavity resonant frequency and quality factor and converts the information into the complex permittivity of the MUT. Finally, the measurement results are displayed in a variety of graphical formats, or saved to disk. The dielectric properties of water layer which depends on temperature are depicted in Fig. 5. The dielectric properties of saturated porous packed bed that composes of glass beads filled with water which depends on temperature are depicted in Fig. 6. Table 1 summaries the dielectric properties of materials, i.e., glass beads and effective value of saturated porous packed bed. The penetration depths following Eq. (2) for each sample (water layer and saturated porous packed bed) at specified condition are summarized in Tables 1 and 2.

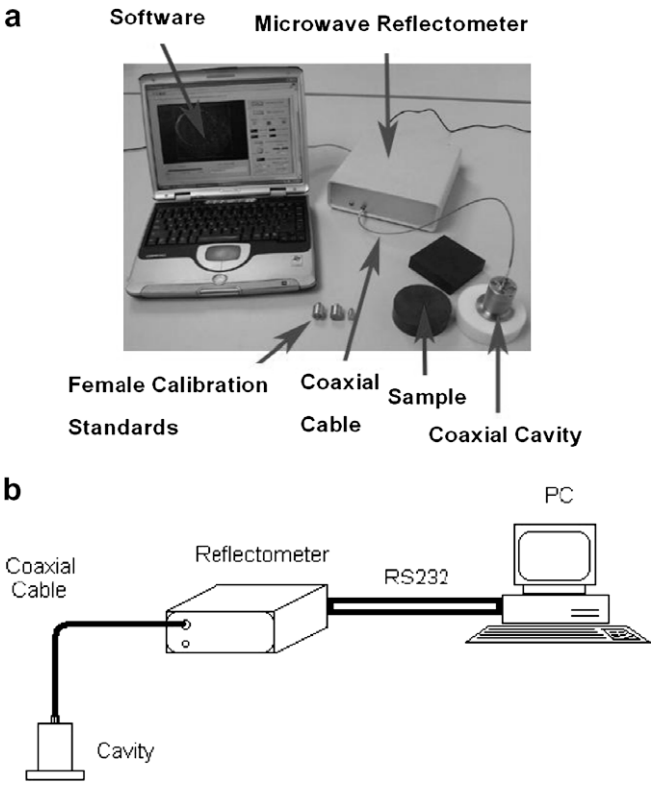

Fig. 3. Portable dielectric measurement (Network Analyzer).

4. Results and discussion

In this section, effects of various parameters on microwave-heating process are investigated. Effects of controlled parameters include microwave power, dielectric properties of sample, dimension and position of sample, on which the following subsections discuss.

4.1. Effects of microwave powers

Water which is the dielectric material examined is heated. The time evolution of temperature rise at the central position inside the water is shown in Fig. 7 with different values of power input. It is found that power significantly influences the rate of temperature rise. Greater power provides greater heat generation rate inside the medium, thereby increasing the rate of temperature rise. To understand further the power effects, Tables 3–5 contain microwave powers of the incident wave, reflected wave, transmitted wave, and the wave that is reflected from water load. The microwave power is

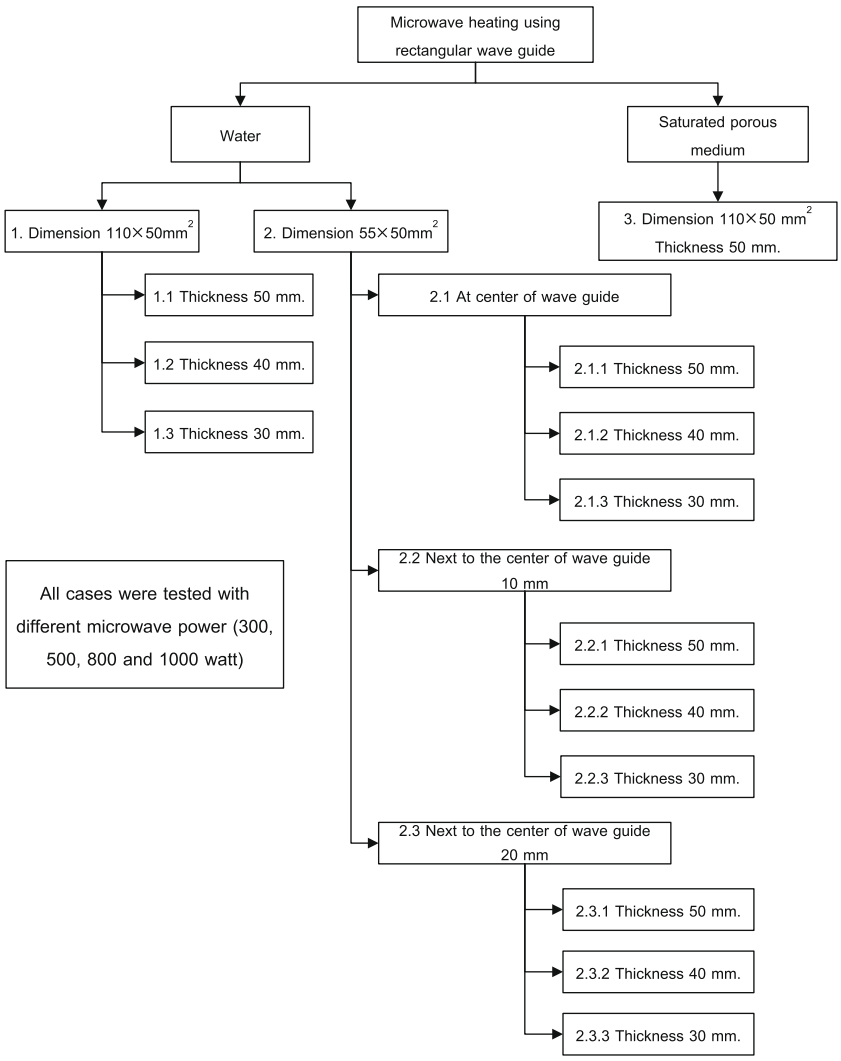

Fig. 4. Test conditions.

detected using a power monitor located at the top and bottom sides of the medium as depicted in Fig. 1c. The power monitor used has accuracy up to two decimal digits. Although the accuracy may not be extremely high, it is adequate for the overall analysis. The microwave powers from the source to a water layer are shown in Tables 3 and 4, respectively, for power of 300 W and 800 W. In addition, Table 5 shows the detected powers applied to a porous bed. It is noticed from Tables 4 and 5 that there is no power that is transmitted can be detected for the power of 300 W while there is some transmitted power when the source power is 800 W. This result indicates that, in the high power case, some waves can transmit through the water layer thereby less amount of power absorbed. This is due to larger penetration dept that results from the decrease in the dielectric properties: relative dielectric constant and loss tangent coefficient. The decrease in dielectric properties is attributed to a higher temperature within the water layer since, for higher power, the electromagnetic field is more intense. Accordingly, volumetric heat generation rate is increased, and thereafter the absorbed energy is converted to more thermal energy. Furthermore, the amount of power transmitted can be detected when the medium is porous because the porous medium has larger penetration dept than that of water due to the effect of different dielectric properties. The reader is directed to the previous work [13] for the detailed investigation of influences of dielectric properties. Temperature change along the z-direction at $X = 55$ mm and $Y = 25$ mm is measured and illustrated in Figs. 8 and 9 for microwave power of 300 W and 800 W, respectively. In both cases, temperature is higher near surface. The case in which power of 800 W is used has greater rate of temperature rise, In addition the temperature is slightly more uniform than that for power 300 W due to greater rate of energy transfer per unit volume.

4.2. Effects of dimensions of material

The following discussions involve investigations of effects of dimensions of material on heating processes. Water in a container with different dimensions is heated by a microwave power of 300 W. Temperatures measured by fiber optic are averaged and recorded. The resulting data is then plotted and shown in Fig. 10. The dimension sizes of container in the x-, y- and z-directions are denoted by X, Y, Z, respectively. It is found that the water that has smaller volume has higher rate change of temperature due to larger heat generation rate per unit volume. However, the exception is observed. Although the water in a $110(X) \times 30(Z) \times 50(Y)$ mm^3 container has larger volume than that in a $55(X) \times 50(Z) \times 50(Y)$ mm^3 container, the water with the larger volume has greater rate of temperature rise. The reason behind this result is that the penetration depth of water that is greater than its thickness causes

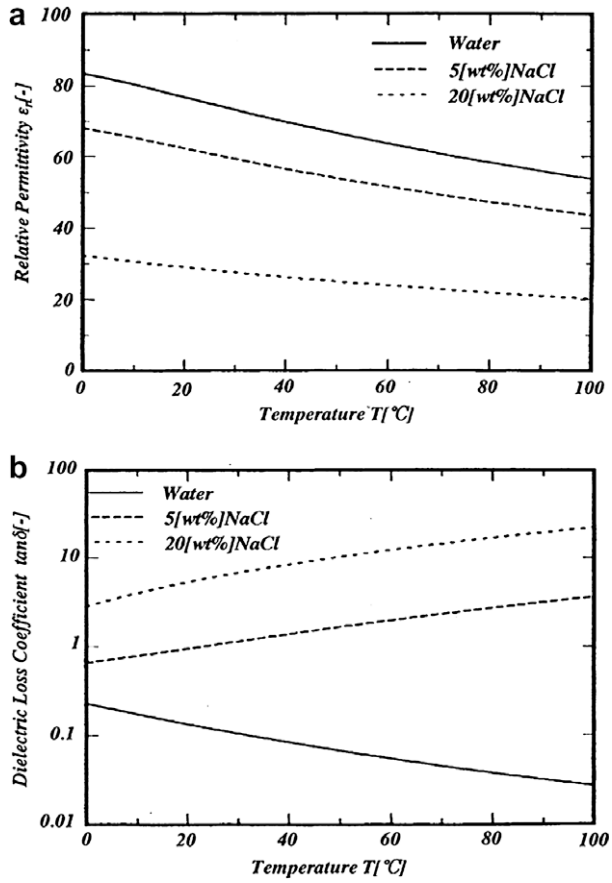

Fig. 5. Dielectric properties of water layered obtained from present study: (a) relative permittivity; (b) loss tangent coefficient.

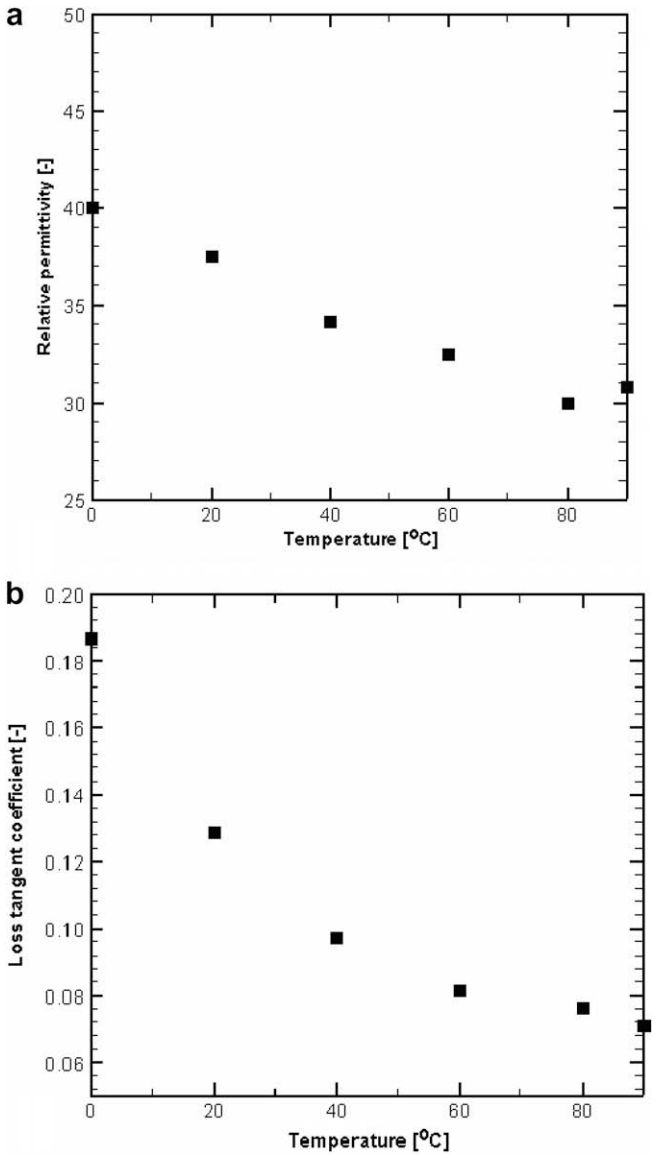

Fig. 6. Dielectric properties of saturated porous medium from experimental: (a) relative permittivity; (b) loss tangent coefficient.

the interference of waves reflected from the interface of water and air at the lower side due to the difference of dielectric properties of water and air. Consequently, the reflection and transmission components at each interface contribute to the resonance of standing wave inside the water sample. Therefore the field distribution does not posses an exponential decay from the surface.

4.3. Effects of positions of sample

In terms of position of sample, the sample which is water with $55(X) \times 50(Z) \times 50(Y)\,\text{mm}^3$ in dimensions is placed in the waveguide at different locations as depicted in Fig. 2c. After the heating time of 120 s, temperature is measured at $X = 27.5$ mm, $Y = 25$ mm, $Z = 50$ mm, and plotted with time in Fig. 11. It can be seen in this figure that the rate change of temperature is highest when location of the sample is shifted to 20 mm away from the center, whereas the rate is lowest when the sample is located at the center. This is caused by stronger resonance effects that occur due to disorder wave reflections. Since sample has its length smaller than the waveguide width, waves reflect disorderly corresponding to a multimode of field pattern.

4.4. Effects of dielectric properties of material

Microwave-heating process within the saturated porous material and water layer are examined in this section. The sample used as the saturated porous material is the porous packed bed filled with uniform glass beads and water. Each glass bead

Table 1
Dielectric properties of water.

Temperature (°C)	Relative permittivity (ε'_r)	Dielectric loss ε''_r	Loss tangent (tan δ)	Penetration depth (D_p)
0	88.1500	38.4725	0.3230	0.012998
20	80.3572	14.3772	0.1789	0.024367
40	73.3916	7.8535	0.1070	0.042523
60	67.0324	5.2186	0.0779	0.061117
80	61.0588	3.7871	0.0620	0.080356
90	58.1476	2.9023	0.0499	0.102305
100	55.2500	1.6630	0.0301	0.174004

Table 2
Dielectric properties of porous packed bead (diameter, $d = 0.15$ mm, porosity, $= 0.385$).

Temperature (°C)	Relative permittivity (ε'_r)	Dielectric loss (ε''_r)	Loss tangent (tan δ)	Penetration depth (D_p)
0	40.0000	7.4720	0.1868	0.0330911
20	37.5000	4.8337	0.1289	0.049416
40	34.1670	3.3244	0.0974	0.068453
60	32.5000	2.6487	0.0816	0.083747
80	30.0000	2.2890	0.0763	0.093193
90	30.8330	2.1891	0.0711	0.098659

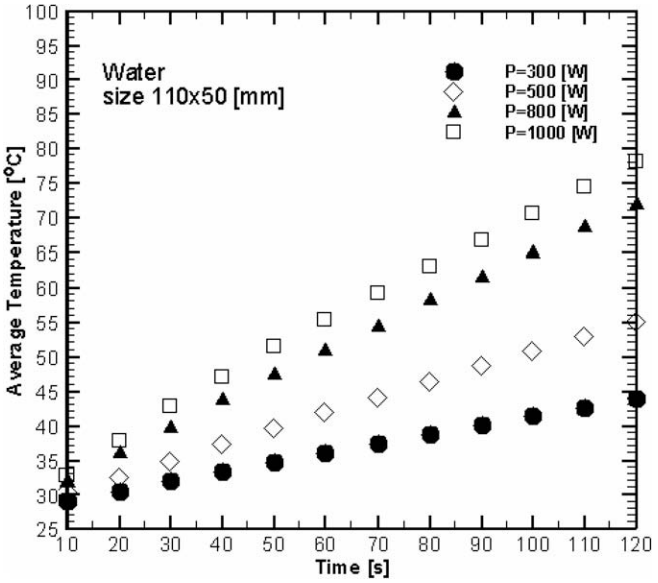

Fig. 7. Distribution of average temperature within water layer as a function of time at various microwave powers.

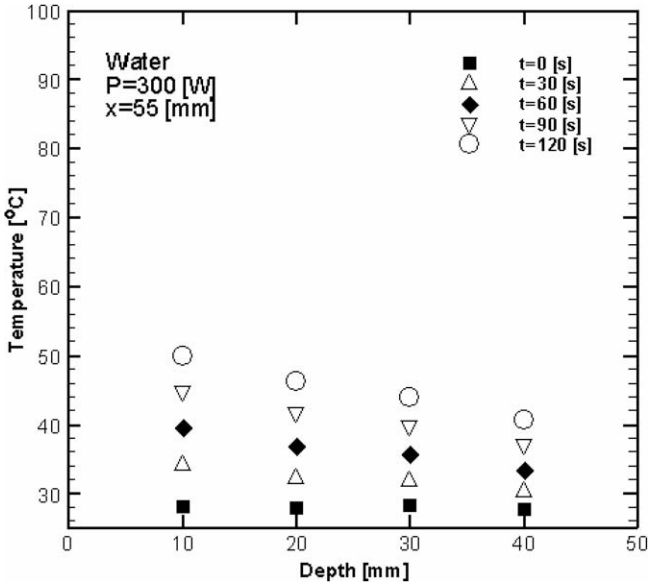

Fig. 8. Distribution of temperature within water layer as a function of distance at various times (P = 300 W, x = 55 mm).

Table 3
Power distribution of water layer size 110 × 50 × 50 mm^3 at 300 W.

Time (s)	Power at top side (W)		Power at bottom side (W)	
	Incident wave (a)	Reflected wave (b)	Transmitted wave (c)	Reflected wave (d)
0	0.30	0.16	0.00	0.00
30	0.30	0.16	0.00	0.00
60	0.30	0.16	0.00	0.00
90	0.30	0.16	0.00	0.00
120	0.30	0.15	0.00	0.00

Table 4
Power distribution of water layer size 110 × 50 × 50 mm^3 at 800 W.

Time (s)	Power at top side (W)		Power at bottom side (W)	
	Incident wave (a)	Reflected wave (b)	Transmitted wave (c)	Reflected wave (d)
0	0.80	0.41	0.00	0.00
30	0.80	0.39	0.01	0.00
60	0.80	0.40	0.02	0.00
90	0.80	0.41	0.04	0.00
120	0.80	0.41	0.05	0.00

Table 5
Power distribution of saturated porous medium size 110 × 50 × 50 mm^3 at 300 W.

Time (s)	Power at top side (W)		Power at bottom side (W)	
	Incident wave (a)	Reflected wave (b)	Transmitted wave (c)	Reflected wave (d)
0	0.30	0.11	0.00	0.00
30	0.30	0.09	0.00	0.00
60	0.30	0.08	0.01	0.00
90	0.30	0.10	0.01	0.00
120	0.30	0.12	0.01	0.00

is 0.15 mm in diameter. For water layer, the temperature profile along the x-direction at the midlength in the y-direction

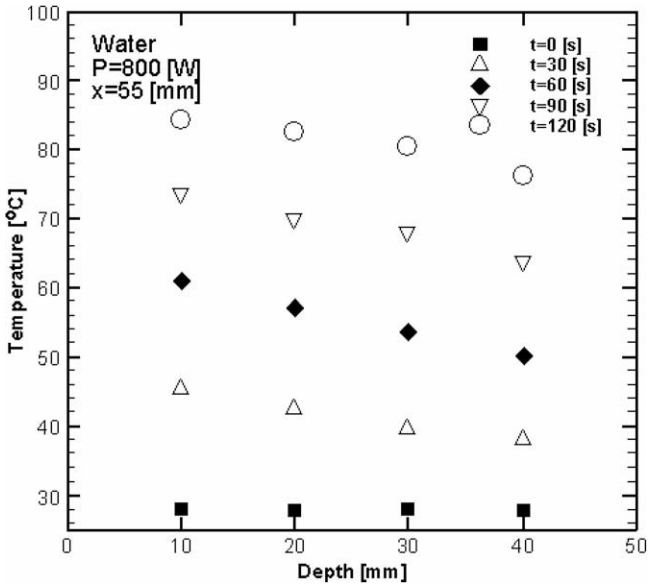

Fig. 9. Distribution of temperature within water layer as a function of distance at various times (P = 800 W, x = 55 mm).

(Y = 25 mm) is shown in Fig. 12 for the heating time of 120 s. The same temperature data in Fig. 12 is also depicted in Fig. 13 as contour lines on the XZ plane in order to see the temperature distribution more clearly. Temperature is highest at the center location since the density of the electric field of the microwave field in the TE_{10} mode is high around the center region in the wave guide. The temperature is higher closer to the surface of water since water is a lossy dielectric material, which has a small penetration depth causing the field to decay rapidly. The penetration depth of water shown in Table 1 is computed using Eq. (2) based on the dielectric properties of water [13]. Next, the result of saturated porous medium can be observed in Figs. 14 and 15, which respectively present the line plots and contours that temperature is high around the bottom region

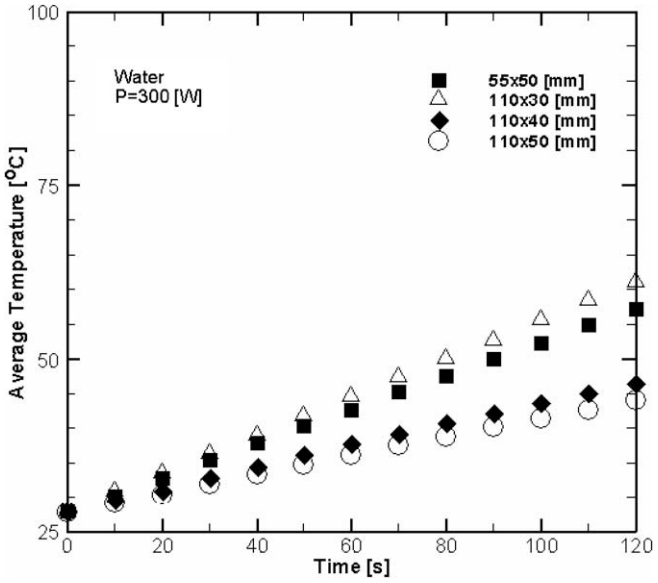

Fig. 10. Distribution of average temperature within water layer as a function of time at various sizes ($P = 300$ W).

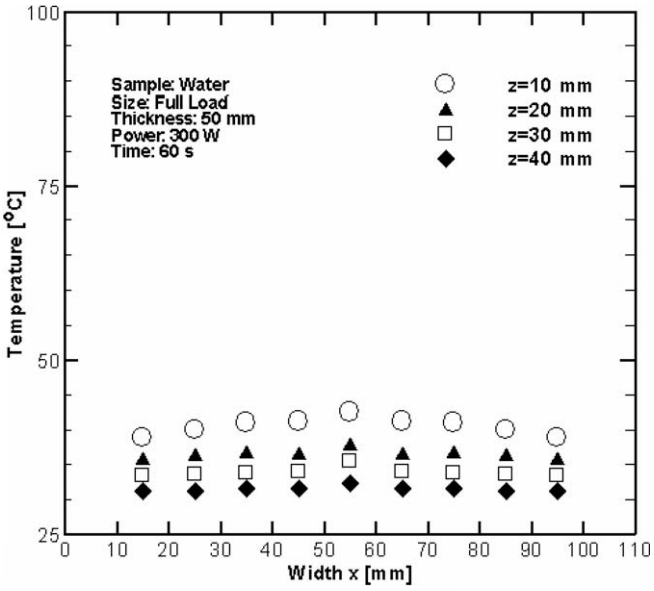

Fig. 12. Distribution of temperature within water layer as a function of distance at various layers.

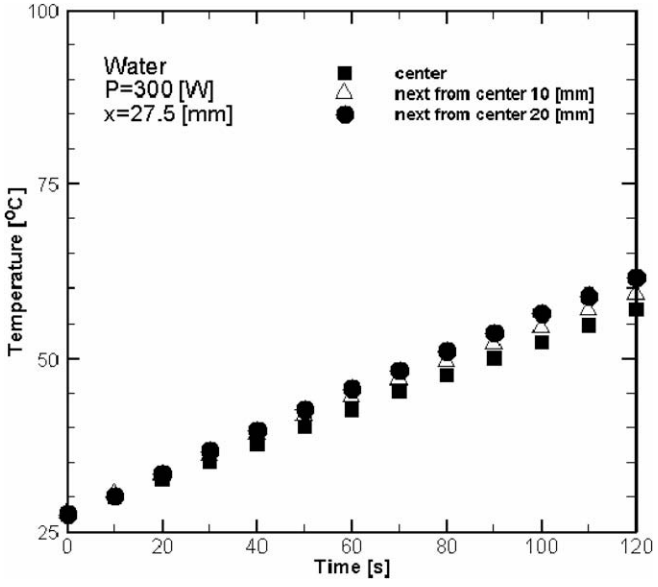

Fig. 11. Distribution of temperature within water layer as a function of time at various positions ($P = 300$ W, $x = 27.5$ mm).

in the packed bed. This porous bed which is considered a low lossy material in which the fields can penetrate much further, causing high temperature region at the bottom of the bed. This is confirmed by a portion of microwave power that penetrates out of the bottom surface of the bed, as shown in Table 5. In contrast, much less power goes through the bottom surface to air as shown in Table 3. Further, the temperature distribution of porous bed (Fig. 14) and water (Fig. 12) are compared. It is found that temperature in the *XZ* plane is more uniform in water than that in porous bed since more convection mechanism exists in water, while conduction is dominant in the porous bed due to minimal flow activities. The flow motions that occur are induced by buoyancy force due to the existence of lateral temperature gradients. To better understand the heat transfer mechanisms within the sample, the time evolution of temperature profile at $Z = 10$ mm is plotted in Fig. 16. It is found that the range of temperature is substantially wider as compared to the case of water sample shown in Fig. 17. In this case, fluid motion is suppressed due to reduced permeability of porous bed. Consequently, the fluid is nearly stagnant indicating that conduction is a dominant mode of heat transfer.

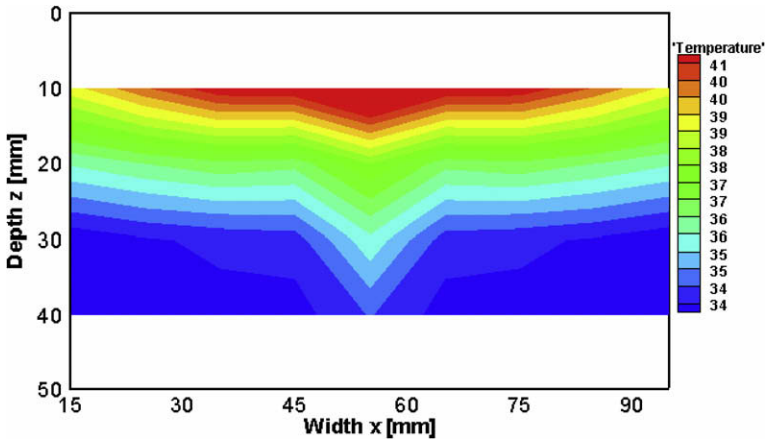

Fig. 13. Distribution of temperature within water layer as a function of distance.

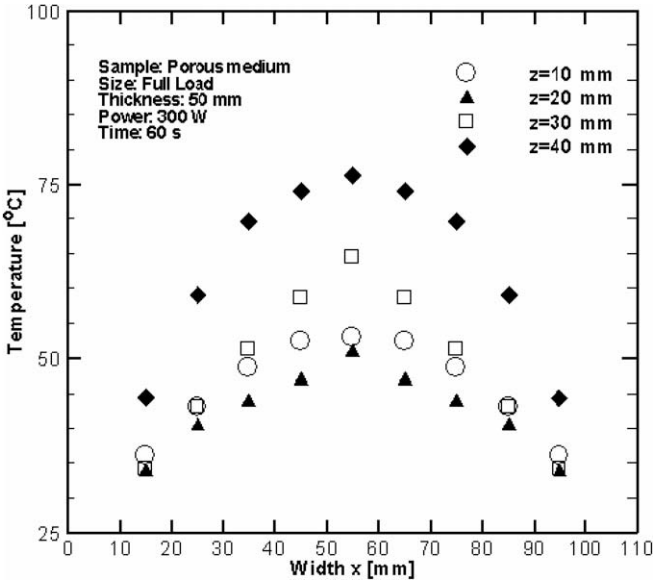

Fig. 14. Distribution of temperature within porous packed bed as a function of distance at various layers.

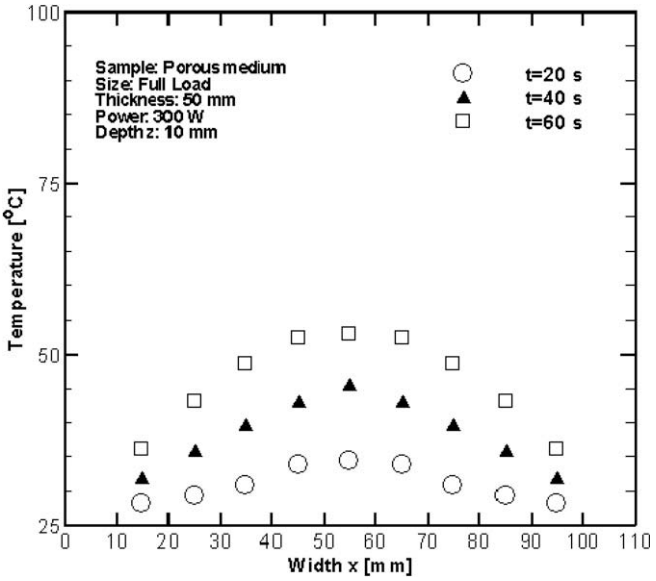

Fig. 16. Distribution of temperature within porous packed bed as a function of distance at various times (P = 300 W, z = 10 mm).

5. Conclusions

The experimental analysis is presented in this paper, which describes many of important behaviors within dielectric materials during microwave heating. Based on the obtained results in the present study, findings can be summarized as follows:

1. Greater power provides greater heat generation rate inside the medium, according to the fact that the electromagnetic heat generation is proportional to the electric intensity to the power of two. As a result, greater power causes greater rate of temperature rise which affects the change in dielectric properties of materials.
2. The sample that has smaller volume has higher rate change of temperature due larger heat generation rate per unit volume. Sample with smaller thickness in the direction of the wave incident has higher rate of an increase in temperature. Within the smaller-thickness sample, the reflection and transmission components at each interface contribute to a stronger resonance of standing wave inside the sample.
3. Since the porous packed bed has its penetration depth much larger than that of water, the electromagnetic fields can pene-

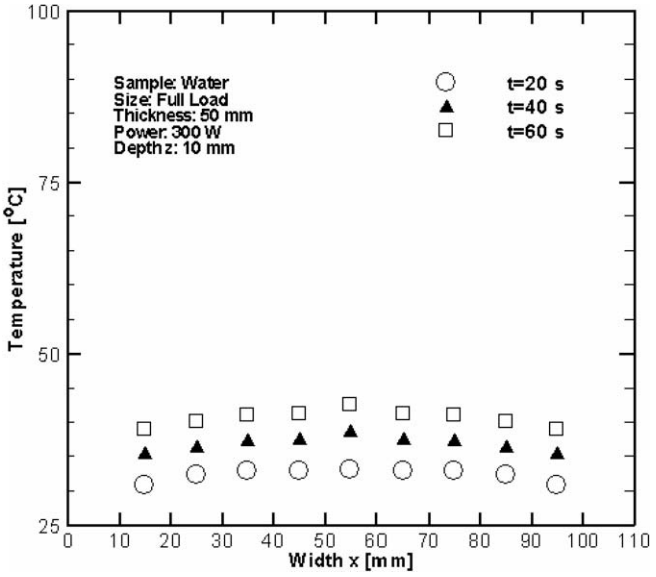

Fig. 17. Distribution of temperature within water layer as a function of distance at various times (P = 300 W, z = 10 mm).

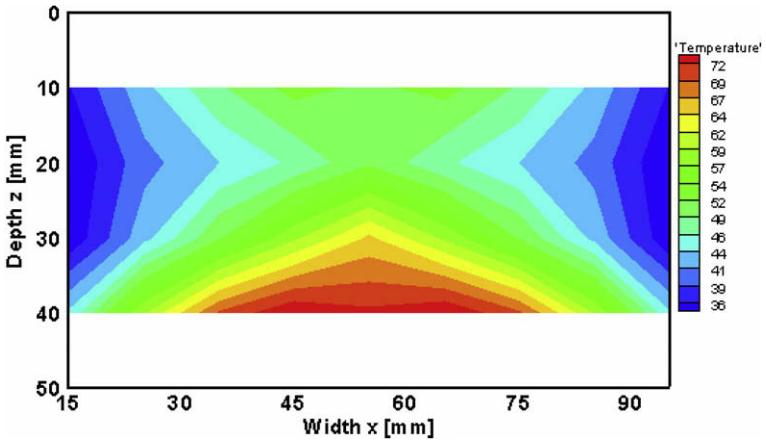

Fig. 15. Distribution of temperature within porous packed bed as a function of distance.

trate much further, resulting in high temperature region at the bottom of the bed.

4. Convection due to buoyancy forced flows which is induced by lateral temperature gradient is considerable in water. However, in case of porous bed, conduction prevails due to minimal flow activities caused by the retarding effect within the bed.

The next steps in research in this problem will be to develop the mathematical model to verify the experimental data.

Acknowledgments

The authors are pleased to acknowledge Thailand Research Fund (TRF) for supporting this research work.

References

[1] A.C. Metaxas, R.J. Meridith, Industrial Microwave Heating, Peter Peregrinus Ltd., London, 1983.
[2] C. Saltiel, A.K. Datta, Heat and mass transfer in microwave processing, Adv. Heat Transfer 30 (1997) 1–94.
[3] K.G. Ayappa, S. Brandon, J.J. Derby, H.T. Davis, E.A. Davis, Microwave driven convection in a square cavity, AIChE J. 31 (5) (1985) 842–848.
[4] J. Clemens, C. Saltiel, Numerical modeling of materials processing in microwave furnaces, Int. J. Heat Mass Transfer 39 (8) (1996) 1665–1675.
[5] D.C. Dibben, A.C. Metaxas, Frequency domain vs. time domain finite element methods for calculation of fields in multimode cavities, IEEE Trans. Magn. 33 (2) (1997) 1468–1471.
[6] H. Zhao, I.W. Turner, The use of a coupled computational model for studying the microwave heating of wood, Appl. Math. Model. 24 (2000) 183–197.
[7] J.R. Bows, M.L. Patrick, R. Janes, A.C. Metaxas, Microwave phase control heating, Int. J. Food Sci. Technol. 34 (1999) 295–304.
[8] H. Zhao, I.W. Turner, G. Torgovnikov, An experimental and numerical investigation of the microwave heating of wood, J. Microwave Power Electromagnet. Energy 33 (1998) 121–133.
[9] J. Watanuki, Fundamental Study of Microwave Heating with Rectangular Wave Guide, M.S. Thesis, Nagaoka University of Technology, Japan, 1998 (in Japanese).
[10] T. Basak, K.G. Ayappa, Influence of internal convection during microwave thawing of cylinders, AIChE J. 47 (2001) 835–850.
[11] P. Ratanadecho, K. Aoki, M. Akahori, Influence of irradiation time, particle sizes and initial moisture content during microwave drying of multi-layered capillary porous materials, ASME J. Heat Transfer 124 (1) (2002) 151–161.
[12] P. Ratanadecho, K. Aoki, M. Akahori, The characteristics of microwave melting of frozen packed bed using a rectangular wave guide, IEEE Trans. Microwave Theory Tech. 50 (6) (2002) 1487–1494.
[13] P. Ratanadecho, K. Aoki, M. Akahori, A numerical and experimental investigation of the modeling of microwave heating for liquid layers using a rectangular wave guide (effects of natural convection and dielectric properties), Appl. Math. Model. 26 (2002) 449–472.
[14] R.R. Lenz, On the microwave heating of saline solution, Journal of microwave power 15 (2) (1980) 107–111.
[15] A.K. Datta, H. Prosetya, W. Hu, Mathematical modeling of batch heating of liquids in a microwave cavity, J. Microwave Power Electromagnet. Energy 27 (1) (1992) 38–48.
[16] Q. Zhang, T.H. Jackson, A. Ungan, Numerical modeling of microwave induced natural convection, Int. J. Heat Mass Transfer 43 (8) (2000) 2141–2154.
[17] J. Zhu, A.V. Kuznetsov, K.P. Sandeep, Mathematical modeling of continuous flow microwave heating of liquids (effects of dielectric properties and design parameters), Int. J. Therm. Sci. 46 (4) (2007) 328–341.
[18] S. Chatterjee, T. Basak, S.K. Das, Microwave driven convection in a rotating cylindrical cavity: a numerical study, J. Food Eng. 79 (4) (2007) 1269–1279.
[19] P. Rattanadecho, The simulation of microwave heating of wood using a rectangular wave guide: influence of frequency and sample size, Chem. Eng. Sci. 61 (2006) 4798–4811.
[20] T. Basak, K.G. Ayappa, Role of length scales on microwave thawing dynamics in 2D cylinders, Int. J. Heat Mass Transfer 45 (2002) 4543–4559.